

Freezing and Slow Evolution in a Constrained Opinion Dynamics Model

F. Vazquez,^{1,*} P. L. Krapivsky,^{1,†} and S. Redner^{1,‡}

¹*Center for BioDynamics, Center for Polymer Studies,
and Department of Physics, Boston University, Boston, MA, 02215*

We study opinion formation in a population that consists of leftists, centrists, and rightist. In an interaction between neighboring agents, a centrist and a leftist can become both centrists or leftists (and similarly for a centrist and a rightist). In contrast, leftists and rightists do not affect each other. The initial density of centrists ρ_0 controls the evolution. With probability ρ_0 the system reaches a centrist consensus, while with probability $1 - \rho_0$ a frozen population of leftists and rightists results. In one dimension, we determine this frozen state and the opinion dynamics by mapping the system onto a spin-1 Ising model with zero-temperature Glauber kinetics. In the frozen state, the length distribution of single-opinion domains has an algebraic small-size tail $x^{-2(1-\psi)}$ and the average domain size grows as $L^{2\psi}$, where L is the system length. The approach to this frozen state is governed by a $t^{-\psi}$ long-time tail with $\psi \rightarrow 2\rho_0/\pi$ as $\rho_0 \rightarrow 0$.

PACS numbers: 64.60.My, 05.40.-a, 05.50.+q, 75.40.Gb

One of the basic issues in opinion dynamics is to understand how consensus is reached from an initial population of individuals (agents) with diverse opinions. Models for this evolution typically are based on each agent freely adopting a new opinion state in response to the opinions in a local neighborhood [1]. More recently, agent incompatibility – in which agents with sufficiently disparate opinions do not interact – has been found to prevent ultimate consensus from being reached [2, 3]. This incompatibility restriction has a profound effect on the opinion dynamics and the final state of the system. The goal of the present paper is to investigate the role of the constraint on opinion formation within a minimal discrete model for which quantitative results can be obtained.

We consider a ternary-opinion system in which each agent can adopt the opinions of leftist, centrist, and rightist. The agents populate a lattice and in a single microscopic event an agent adopts the opinion of a randomly-chosen neighbor (voter model dynamics [4]). This dynamics is augmented by the crucial feature that leftists and rightists are so incompatible that they do not interact. While a leftist could not become a rightist (and vice versa) in a single step, the evolution leftist \Rightarrow centrist \Rightarrow rightist is possible. These rules are easy to implement on any graph, and the final opinion outcome is either consensus of centrists or a frozen mixture of extremists with no centrists. Fig. 1 gives a typical example of a frozen state on the square lattice (with periodic boundary condition). Notice the existence of nested enclaves of opposite opinions and the clearly visible clustering.

To find the probability that consensus is eventually reached, let us temporarily disregard the difference between leftists and rightists. The corresponding binary

opinion model then reduces to the classical voter model [4] that is known to reach one of the two “absorbing” states: All agents become centrists with probability ρ_0 or become extremists with probability $1 - \rho_0$, where ρ_0 is the initial density of centrists. To understand the nature of the frozen state (Fig. 1) and the approach to this state, we shall focus on the case of one dimension where the frozen state is simply an alternating array of contiguous leftist and rightist domains.

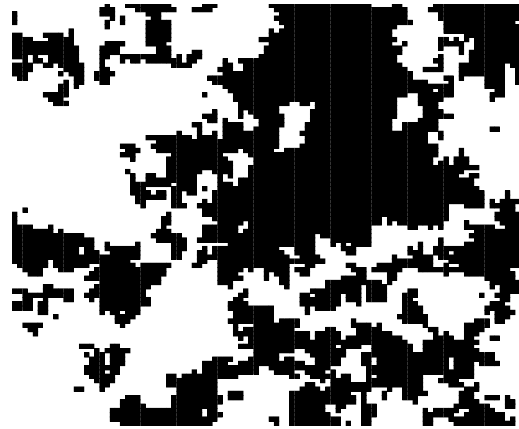


FIG. 1: Snapshot of a typical frozen final state in our opinion dynamics model on a 100×100 square lattice for $\rho_0 = 0.1$. The two extreme opinions are represented by black and white.

There is a fruitful connection between our opinion dynamics model in one dimension and a spin-1 Ising chain endowed with single-spin flip zero-temperature Glauber kinetics [5] in which we regard leftist, centrist, and rightist opinions as the spin states \downarrow , 0 , and \uparrow . This Ising model picture suggests that the best way to analyze the dynamics is to reformulate it in terms of domain walls. There are three types of domain walls: freely diffusing mobile domain walls between $\uparrow 0$ and between $\downarrow 0$, that we denote by M_+ and M_- , respectively, and stationary

*Electronic address: fvazquez@buphy.bu.edu

†Electronic address: paulk@bu.edu

‡Electronic address: redner@bu.edu

domain walls S between $\uparrow\downarrow$. The mobile walls evolve by

$$\begin{aligned} M_{\pm} + M_{\pm} &\rightarrow \emptyset, \\ M_{\pm} + M_{\mp} &\rightarrow S. \end{aligned}$$

When a mobile wall hits a stationary wall, the former changes its sign while the latter is eliminated:

$$M_{\pm} + S \rightarrow M_{\mp}.$$

Thus stationary domain walls are dynamically invisible; their only effect is to change the sign of a mobile wall upon meeting a stationary wall, after which the latter disappears (Fig. 2). The inertness of the stationary walls is reminiscent of the kinetic constraints in models of glassy relaxation. These constraints often give rise to extremely slow kinetics [6, 7, 8, 9]; this feature also occurs in our opinion dynamics model.

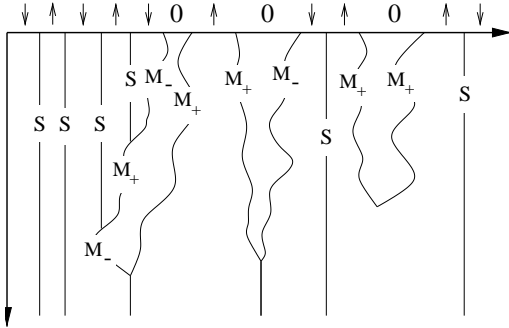


FIG. 2: Space-time representation of the domain wall dynamics. Time runs vertically downward. The spin state of the domains and the identity of each domain wall are indicated.

An important subtlety in the arrangement of domain walls is that an arbitrary initial opinion state necessarily leads to an *even* number of mobile walls between each pair of stationary walls. It is also easy to verify that domain wall sequences of the form $\dots M_+ M_- M_+ \dots$ cannot arise from an underlying opinion state. These topological constraints play a crucial role in the kinetics.

The exact density of mobile walls can be obtained by mapping the constrained spin-1 system onto a spin-1/2 system. In this mapping, we consider both \uparrow and \downarrow spins as comprising the same spin state, while the zero spins comprise the other state. With this identification, the reduced model is just the spin-1/2 ferromagnetic Ising chain with zero-temperature Glauber dynamics and *no* kinetic constraint. In the reduced model, domain walls M_+ and M_- are indistinguishable; they undergo diffusion and annihilate upon colliding. Then the total density of mobile walls $M(t) = M_+(t) + M_-(t)$ is known exactly for arbitrary initial conditions from the original Glauber solution [5]. For initially uncorrelated opinions and if the magnetization of the spin-1/2 system – here the difference between the density of non-zero and zero spins – equals m_0 , then [10]

$$M(t) = \frac{1 - m_0^2}{2} e^{-2t} [I_0(2t) + I_1(2t)], \quad (1)$$

where I_k is the modified Bessel function of index k .

In our original spin-1 system, $m_0 = \rho_{\uparrow} + \rho_{\downarrow} - \rho_0$, or $m_0 = 1 - 2\rho_0$ due to normalization. If the initial densities of \uparrow and \downarrow opinions are equal, then $M_+(t) = M_-(t)$ and the densities of mobile domain walls are

$$\begin{aligned} M_{\pm}(t) &= \rho_0(1 - \rho_0) e^{-2t} [I_0(2t) + I_1(2t)] \\ &\sim \rho_0(1 - \rho_0) (\pi t)^{-1/2}. \end{aligned} \quad (2)$$

As expected, the mobile wall density decays asymptotically as $t^{-1/2}$ because of the underlying diffusive dynamics. However, the density of stationary domain walls $S(t)$ decays algebraically,

$$S(t) \propto t^{-\psi(\rho_0)}, \quad (3)$$

with a *non-universal* exponent (Fig. 3). Naively, one might have expected that the decay of stationary walls could be accounted by persistence [11, 12, 13]; this accounts for the probability that a given lattice site is not hit by any diffusing domain wall. For the kinetic spin-1/2 Ising model, this persistence probability decays as $t^{-\theta}$, with $\theta = 3/8$ [14], independent of the initial domain wall density, if the walls are initially uncorrelated.

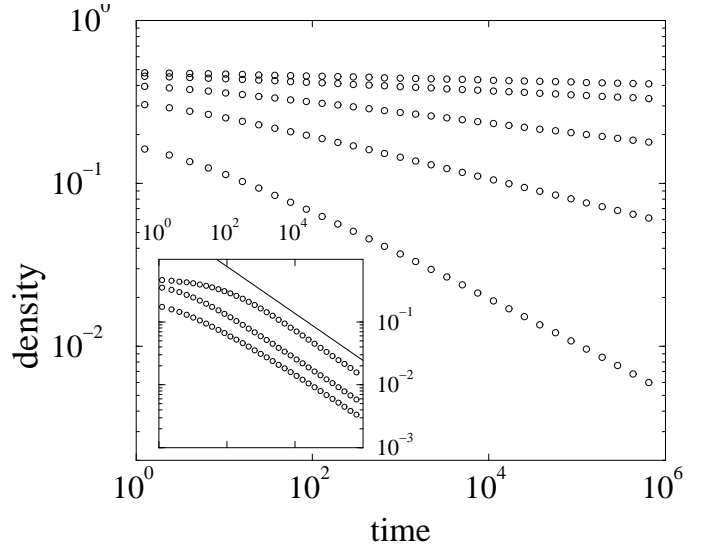


FIG. 3: Density of stationary domain walls versus time on a double logarithmic scale for the initial conditions $\rho_0 = 0.02, 0.04, 0.10, 0.20$, and 0.40 (top to bottom). The respective exponent estimates are $0.013, 0.026, 0.065, 0.13$, and 0.20 . Data are based on 100 realizations of a chain with 5×10^5 sites. Inset: Stationary domain wall density for initially uncorrelated walls based on the same amount of data. Shown are the cases $\rho_0 = 0.02, 0.10$, and 0.40 (top to bottom). The solid line has slope $-3/8$.

To check this striking result for ψ , we also simulated a system with spatially uncorrelated domain walls. While such a domain wall state cannot arise from any initial opinion state, we can prepare directly an uncorrelated arrangement of domain walls with prescribed densities.

For any initial condition in this test system, the stationary wall density decays as $t^{-3/8}$ (inset to Fig. 3), consistent with persistence [11, 12]. Thus the topological constraints imposed on the domain wall arrangement in our opinion dynamics model appear to control the dynamics.

The physical origin of the slow decay in the density of stationary domain walls stems from the dependence of the amplitude in the mobile wall density on the initial condition (Eq. (2)). This dependence arises because of the pairing of mobile domain walls in the initial state when ρ_0 is small. For $\rho_0 \rightarrow 0$, each pair becomes independent and their survival probability is proportional to their initial (unit) separation [15]. In contrast, the amplitude is independent of ρ_0 for randomly distributed walls. We now exploit this observation to estimate the density of stationary walls as $\rho_0 \rightarrow 0$. In this limit, the system initially consists of long strings of stationary domain walls that are interspersed by a pair of mobile domain walls. According to Eq. (2), the asymptotic density of mobile domain walls is $M \sim 2\rho_0/\sqrt{\pi t}$. Within a rate-equation approximation, the density of stationary domain walls decays according to

$$\dot{S} = -k M S. \quad (4)$$

While such a rate equation is generally inapplicable in low spatial dimension, we can adapt it to one dimension by taking an effective time-dependent reaction rate $k \sim \sqrt{2/\pi t}$ [12, 15]. This is just the time-dependent flux to an absorbing point due to a uniform initial background of diffusing particles; such a rate phenomenologically accounts for effects of spatial fluctuations in one dimension. Substituting the asymptotic expression for $M(t)$ from Eq. (1) and the above reaction rate into this rate equation, we find that the density of stationary walls decays as $t^{-\psi}$ with $\psi(\rho_0) = \sqrt{8}\rho_0/\pi$ as $\rho_0 \rightarrow 0$.

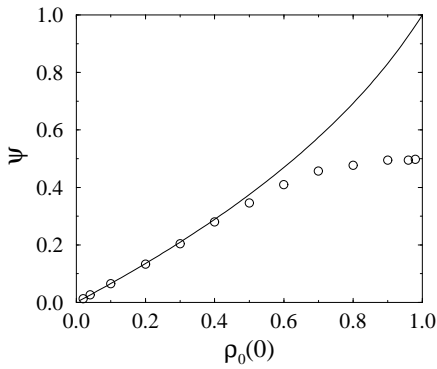


FIG. 4: Comparison of the exponent ψ from Eq. (5) and from the simulation data of Fig. 3 (circles).

Perhaps a more compelling way to determine $\psi(\rho_0)$ is through a relation with persistence in the q -state Potts model. Because the initial magnetization in the reduced spin-1/2 system is $m_0 = 1 - 2\rho_0$, it has been argued (see

[16]) that this system should be identified with the q -state Potts model with $m_0 = 2/q - 1$, or $q = (1 - \rho_0)^{-1}$. Using the exact persistence exponent for the q -state Potts model with Glauber kinetics [14], and identifying ψ with this persistence exponent, we obtain

$$\psi(\rho_0) = -\frac{1}{8} + \frac{2}{\pi^2} \left[\cos^{-1} \left(\frac{1 - 2\rho_0}{\sqrt{2}} \right) \right]^2. \quad (5)$$

This has the limiting behavior $\psi(\rho_0) \rightarrow 2\rho_0/\pi$ as $\rho_0 \rightarrow 0$.

This asymptotics is in excellent agreement with our numerical results for $\rho_0 \lesssim 0.4$ (Fig. 4) but then deviates for larger ρ_0 , where Eq. (5) predicts $\psi > 1/2$ while $\psi(\rho_0)$ must monotonically approach 1/2 as $\rho_0 \rightarrow 1$. It should also be noted that in this identification with persistence, we have ignored the creation of new stationary interfaces due to the meeting of opposite mobile domains M_+ and M_- . This creation process occurs with a rate of the order of $(-dS/dt)_{\text{gain}} \propto t^{-3/2}$. If $\psi < 1/2$, this creation term is subdominant and can thus be ignored [17].

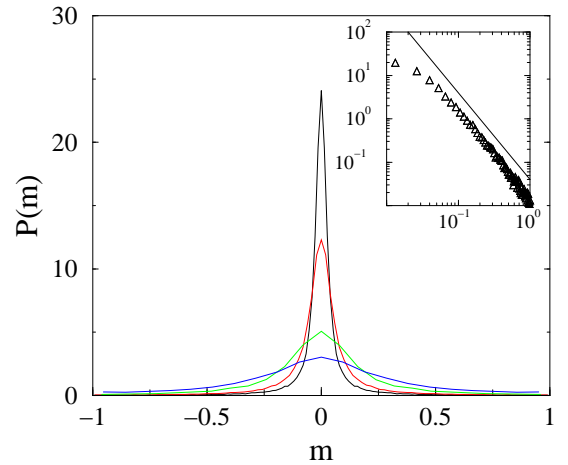


FIG. 5: Magnetization distribution $P(m)$, with $m = \rho_\uparrow - \rho_\downarrow$, in the frozen final state for the cases $\rho_0 = 0.02$ (10^5 realizations), 0.04, 0.1, and 0.2 (10^4 realizations) on a 5000 site linear chain. Inset: $P(m)$ for $\rho_0 = 0.02$ on a double logarithmic scale to illustrate the m^{-2} tail. The straight line has slope -2 .

An important characteristic of the system is the spatial arrangement of domain walls. The mean distances between nearest-neighbor MM and MS pairs both appear to grow as $t^{1/2}$ due to the diffusive motion of mobile domain walls. The distributions of these two distances both obey scaling, with scaling function of the form ze^{-z^2} , where $z = x(t)/\langle x(t) \rangle$ is the scaled distance. In contrast, the distances between neighboring stationary walls x_S appear to be characterized by two length scales. There are large gaps of length of the order of $t^{1/2}$ that are cleared out by mobile domain walls before they annihilate (Fig. 2). However, there are also many very short distances remaining from the initial state. The corresponding moments $M_k(t) \equiv \langle x_S^k(t) \rangle^{1/k}$ reflect this multiplicity of scales, with $M_k(t)$ approaching a $t^{1/2}$ growth

law as $k \rightarrow \infty$, while M_k grows extremely slowly in time for $k \rightarrow 0$.

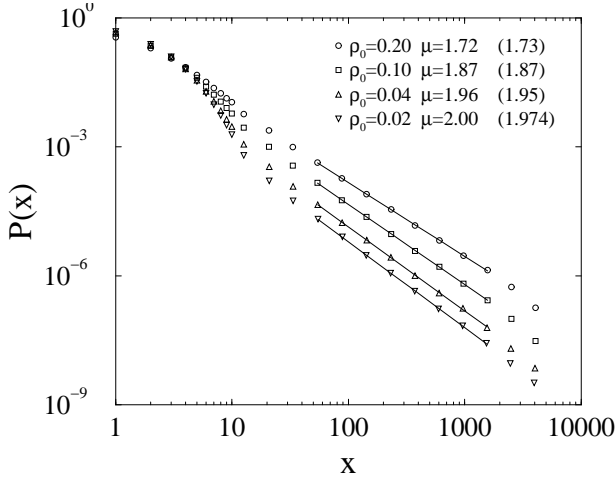


FIG. 6: Domain length distribution $P(x)$ in the frozen final state for the same parameters and number of realizations as in Fig. 5. The data have been binned over a small logarithmic range to reduce fluctuations. Tabulated are the slopes from each data set and the expected value $2(1 - \psi)$ (parentheses) from our simulation result for ψ .

Eventually all the mobile domain walls disappear and the final state consists of centrists (this happens with probability ρ_0) or a frozen mixture of extremists. The frozen state has magnetization distribution $P(m)$ (density difference of \uparrow and \downarrow spins) that broadens as ρ_0 increases (Fig. 5). This reflects the fact that there is progressively more evolution before the system ultimately freezes. For small ρ_0 , $P(m)$ has a m^{-2} tail. To explain this result, consider the evolution of a single pair of mobile walls. This pair annihilates at time t with prob-

ability density $\Pi(t) \propto t^{-3/2}$. The total magnetization of the resulting frozen state scales as $t^{1/2}$ since the domain wall pair annihilates at a distance $x \propto t^{1/2}$ from its starting point. Then from $P(m) dm = \Pi(t) dt$, together with $\Pi(t) \propto t^{-3/2}$ and $m \propto \rho_0 t^{1/2}$, we indeed obtain $P(m) \propto \rho_0 m^{-2}$.

The domain length statistics in the frozen state reflects the opinion evolution. The frozen state is reached when $t = T_f \propto L^2$; this is the time needed for mobile walls to diffuse throughout the system and thus be eliminated. At this time, the density of stationary walls is of the order of $S \propto T_f^{-\psi} \propto L^{-2\psi}$. Thus the average length of single-opinion domains is $\langle x \rangle \propto L^{2\psi}$. Numerically we find that the domain length distribution has a power law tail, $P(x) \propto x^{-\mu}$ with $1 < \mu < 2$. The lower bound ensures normalizability while the upper bound implies that $\langle x \rangle$ diverges as $L \rightarrow \infty$. From the above power law form, $\langle x \rangle = \int dx x P(x) \propto L^{2-\mu}$. This matches our previous estimate $\langle x \rangle \sim L^{2\psi}$ when $\mu = 2(1 - \psi)$. Fig. 6 shows the length distribution of single-opinion domains in the frozen state. Direct estimates of the exponent μ from this plot are in good agreement with the exponent relation $\mu = 2(1 - \psi)$, with ψ obtained from the time dependence of the mobile wall density in Fig. 3.

In summary, the constraint that extremists with opposite opinions cannot influence each other leads to a rich opinion dynamics that becomes extremely slow when the initial density ρ_0 of centrists is small. With probability $1 - \rho_0$ the population evolves to a static state that consists of extremist enclaves. Perhaps this simple picture can account for the sad phenomenon of the proximity of incompatible populations in too many locations around the world.

We thank S. Majumdar for helpful correspondence. We are grateful to NSF grant DMR9978902 for partial support of this work.

[1] H. Föllmer, *J. Math. Econ.* **1**, 51 (1974); J. Kobayashi, *J. Math. Sociology* **24**, 285 (2001); R. Hegselmann and U. Krause, *J. Artif. Soc. Soc. Simul.* **5**, no. 3 (2002) and references therein.

[2] B. Latanaé and A. Nowak, in *Progress in Communication Science*, pp. 43, eds. G. A. Barnett and F. J. Boster.

[3] G. Weisbuch, G. Deffuant, F. Amblard, and J. P. Nadal, *cond-mat/0111494*.

[4] T. M. Liggett, *Interacting Particle Systems* (Springer-Verlag, New York, 1985).

[5] R. J. Glauber, *J. Math. Phys.* **4**, 294 (1963).

[6] J. Jackle and S. Eisinger, *Z. Phys. B* **84**, 115 (1991).

[7] P. Sollich and M. R. Evans, *Phys. Rev. Lett.* **83**, 3238 (1999).

[8] S. N. Majumdar, D. S. Dean, and P. Grassberger, *Phys. Rev. Lett.* **86**, 2301 (2001).

[9] A. Crisanti, F. Ritort, A. Rocco, and M. Sellitto, *cond-*

mat/0109302.

[10] J. G. Amar and F. Family, *Phys. Rev. A* **41**, 3258 (1990).

[11] B. Derrida, A. J. Bray, and C. Godrèche, *J. Phys. A* **27**, L357 (1994).

[12] P. L. Krapivsky, E. Ben-Naim, and S. Redner, *Phys. Rev. E* **50**, 2474 (1994).

[13] D. Stauffer, *J. Phys. A* **27**, 5029 (1994).

[14] B. Derrida, V. Hakim, and V. Pasquier, *Phys. Rev. Lett.* **75**, 751 (1995).

[15] S. Redner, *A Guide to First-Passage Processes*, (Cambridge University Press, New York, 2001).

[16] C. Sire and S. N. Majumdar, *Phys. Rev. E* **52**, 244 (1995).

[17] A similar feature occurs in a cyclic 4-state voter model; see L. Frachebourg, P. L. Krapivsky, and E. Ben-Naim, *Phys. Rev. E* **54**, 6186 (1996).